Pair production of $W^{\pm}$, γ, and Z in association with jets

V. Barger, T. Han, and D. Zeppenfeld
Physics Department, University of Wisconsin, Madison, Wisconsin 53706

J. Ohnemus
Physics Department, Florida State University, Tallahassee, Florida 32306
(Received 22 November 1989)

Amplitudes for the production of electroweak-gauge-boson pairs (any combination of γ, Z, or $W^{\pm}$) in association with up to two jets are given. The gauge bosons may be either real or virtual with subsequent decays into charged or neutral leptons. The amplitudes are presented in a form directly amenable to numerical evaluation. Representative cross sections are given for Fermilab Tevatron, CERN Large Hadron Collider, and Superconducting Super Collider center-of-mass energies.

I. INTRODUCTION

The standard model (SM) of strong and electroweak interactions has been amazingly successful in the past in describing a large variety of experimental data. This success makes it even more imperative to test additional processes for possible discrepancies between theory and experiment, in order to unravel possible first hints for new physics. Since one of the major open questions in the SM concerns the nature of electroweak-symmetry breaking, the production of electroweak bosons at e^+e^-, $p\bar{p}$, pp, and ep colliders[1-5] is deserving of further scrutiny.

Recently extensive studies have been performed of W, Z, and photon production in association with up to three jets,[6-9] which are of immediate interest for both the CERN and Fermilab $p\bar{p}$ collider experiments. Considerable theoretical work has been done in the past on W^+W^- production at e^+e^- colliders,[3] on W^+W^-, ZZ, $W^{\pm}Z$, and $W^{\pm}\gamma$ production at hadron colliders[2,4,10] and on $W^{\pm}$+1-jet production in ep collisions[5,11] which will for the first time allow a direct test of the electroweak three-gauge-boson couplings, a test which is needed to confirm the non-Abelian gauge structure of the electroweak interactions. Previous work on V_1V_2+1-jet production at hadron colliders ($V=W,Z,\gamma$) includes complete calculations of one-loop radiative corrections to $\gamma\gamma$ (Ref. 12) and $W\gamma$ (Ref. 13) cross sections and tree-level results for the general one-jet case.[14]

In this paper we derive theoretical expressions for V_1V_2+2-jet cross sections at hadron colliders, which are important to obtain a more precise picture of the jet activity in vector-boson pair production. Perhaps even more important is a precise understanding of these processes as a background to new-physics searches. A partial list of applications for such a V_1V_2+2-jet study is easily enumerated.

(1) The production of heavy-top-quark pairs leads to final states with two W's and two jets:[15] $p\bar{p}\to t\bar{t}\to W^+bW^-\bar{b}$. For very large top-quark masses, $m_t > 150$ GeV, say, the WW+2-jet background may become significant.

(2) In studies of W^+W^- production, aimed at measuring the $WW\gamma$ and WWZ vertices, one needs to know the typical jet activity in these events in order to distinguish them from $t\bar{t}$ production with subsequent decay into real W's. Without such a study, $p\overset{(-)}{p}\to W^+W^-X$, which could be the most powerful reaction for analyzing the three-gauge-boson vertex in future collider runs,[10] would not be useful.

(3) The principal production mechanism for a heavy Higgs boson ($m_H \gtrsim 0.6$ TeV) is via W-boson fusion where the two quarks which radiate the almost real W's are in principle detectable as two high-rapidity jets. With the subsequent $H\to ZZ$ decay, the process $pp\to ZZ$+2 jets that we calculate is an irreducible physics background which needs to be understood, if one wants to tag the jets in Higgs-boson events at the CERN Large Hadron Collider (LHC) or Superconducting Super Collider (SSC). Jet tagging may be a useful tool for reducing backgrounds from $q\bar{q}\to ZZ$ events.[16]

(4) A variety of new-physics sources leads to multiple weak bosons and jets in the final state. One example is the cascade decays of squarks and gluinos.[17] Clearly it is desirable to know the SM rates for such events in order to unambiguously identify the new-physics signals.

In this paper we present a perturbative calculation of production cross sections for electroweak-boson pairs V_1V_2 ($V_i=W,Z,\gamma$) in association with up to two jets. Analogous calculations already exist for V_1V_2 production in association with 0 or 1 jet,[14] but for V_1V_2+2-jet production only partial calculations exist in the literature.[18] In particular the subprocesses involving external gluons have not been previously calculated.

For problems involving large numbers of Feynman graphs the direct numerical evaluation of amplitudes corresponding to fixed initial- and final-state polarizations and subsequent quadrature and summation over helicities is the method of choice. A variety of methods has been developed in the past to obtain analytic formulas for heli-

city amplitudes.[19–22] In a problem of complexity similar to the present one, namely, W or Z production in association with three jets at $p\bar{p}$ colliders, it was found that the amplitude calculus developed in Ref. 22 yields a very efficient code for the evaluation of cross sections and we employ this particular method in this paper. In general, when doing calculations with amplitude techniques for weak-boson production it is straightforward to include the decay of the weak bosons to final-state leptons and interference effects between photon and Z exchange diagrams, which in the end allows one to determine the full correlations among weak-boson decay products.

The amplitude formulas to be presented below have very simple crossing relations which allow us to relate a variety of processes. The basic calculations which we have carried out are analytic expressions for the $q\bar{q}V_1V_2gg$ and $q\bar{q}V_1V_2q\bar{q}$ amplitudes which are relevant for pair production of electroweak bosons in $p\overset{(-)}{p}$ collisions via the subprocesses

$$q\bar{q}\to V_1V_2gg\ , \tag{1.1a}$$

$$qg\to V_1V_2qg\ , \tag{1.1b}$$

$$g\bar{q}\to V_1V_2\bar{q}g\ , \tag{1.1c}$$

$$gg\to V_1V_2q\bar{q}\ , \tag{1.1d}$$

and

$$q\bar{q}\to V_1V_2q\bar{q}\ , \tag{1.2a}$$

$$qq\to V_1V_2qq\ , \tag{1.2b}$$

$$\bar{q}\,\bar{q}\to V_1V_2\bar{q}\,\bar{q}\ . \tag{1.2c}$$

When the V leptonic decays ($\gamma,Z\to e^+e^-$ or $W\to e\nu$) are included the same amplitudes yield, by crossing, the parton-level cross sections for $ep\to e(\nu)+3$-jet production, arising, e.g., from

$$eq\to lV_2qgg \tag{1.3}$$

via V_1 exchange, which is crossing related to the processes of Eq. (1.1).

The primary intent of this paper is to set up amplitude and cross-section formulas for V_1V_2+n-jet production ($n=0,1,2$). We also address some illustrative phenomenological applications. We evaluate the V_1V_2+n-jet cross sections in $p\bar{p}$ collisions at the Fermilab Tevatron and in pp collisions in LHC and SSC energies, for $n=0$, 1, and 2 jets with typical jet acceptance criteria. We also discuss $\gamma\gamma+n$-jet production in $p\bar{p}$ collisions at the Tevatron in some detail.

The remainder of this paper is organized as follows. In Sec. II we derive analytic expressions for the $q\bar{q}V_1V_2gg$ and $q\bar{q}V_1V_2q\bar{q}$ amplitudes. For the sake of completeness and to familiarize the reader with our notation we also include expressions for $q\bar{q}V_1V_2$ and $q\bar{q}V_1V_2g$ amplitudes, which correspond to V_1V_2 and V_1V_2+1-jet production in hadron collisions. A special subsection is devoted to the generalization of the formulas when one wants to include the decay of the electroweak bosons V_1 and V_2. Section III contains the phenomenological discussion mentioned above, while technical details have been relegated to three appendixes. Appendix A presents a self-contained summary of the amplitude calculus of Ref. 22 and sets up the notation used in Sec. II. In Appendix B the handling of color factors is explained and finally, in Appendix C we explain briefly how to assemble our amplitudes into parton-level cross-section formulas.

II. VV AMPLITUDES

In this section we give the helicity amplitudes for the production of weak-boson pairs plus n jets ($n=0,1,2$). The amplitudes are evaluated using the methods described in Ref. 22. The notation is explained in detail in Appendix A.

Basically we derive analytic expressions for scattering amplitudes in the two-component Weyl basis for the spinors. Products of Dirac matrices $\not{a}=a_\mu\gamma^\mu$ and spinors then reduce to two-by-two matrix multiplication of Pauli matrices $(\not{a})_{\pm}=a^0\mp\mathbf{a}\cdot\boldsymbol{\sigma}$ and two-component Weyl spinors $\langle i|$ and $|j\rangle$, which is performed numerically in the end. The task is then to rewrite all amplitudes in two-component notation, simplifying the expressions on the way and factorizing components common to several Feynman graphs whenever possible. In order to exploit the great simplifications that occur in the relativistic limit, we set all fermion masses equal to zero throughout this paper.

In presenting the formulas for the amplitudes the fermion momenta p_i ($i=1,2,\ldots$) are chosen to point in direction of the arrow of the fermion line (p_1 is incoming and p_2 is outgoing in all the diagrams). All boson momenta (k_i for V_i, g_i for gluons) are chosen to be outgoing. For a given process the momenta of the physical particles may differ by a sign from the momenta appearing in the corresponding Feynman diagrams and the set of sign factors for all external particles suffices to completely specify any of the scattering processes related by crossing. We will denote the physical momentum of a particle by a bar over the momentum that appears in the Feynman diagrams. For fermions we thus have

$$p_i=S_i\bar{p}_i \tag{2.1}$$

with $S_i=+$ for quarks and $S_i=-$ for antiquarks. Similarly we distinguish the chirality indices σ_i and the physical helicities $\bar{\sigma}_i/2$:

$$\sigma_i=S_i\bar{\sigma}_i\ . \tag{2.2}$$

We will use the physical momenta $(\bar{p}_i,\bar{g}_i,\bar{k}_i)$ and physical helicities $\bar{\sigma}_i/2$ to express the phase space and the wave functions of fermions and bosons, whereas we employ the momentum flow as appearing in the Feynman diagrams (p_i,g_i,k_i) and the chirality indices σ_i to express truncated amplitudes.

A. $VVqq$

Weak-boson pair production with no jets is described by the $VVqq$ process shown in Fig. 1. The triple-weak-boson vertex ($V\to V_1V_2$) is introduced through the four-vector

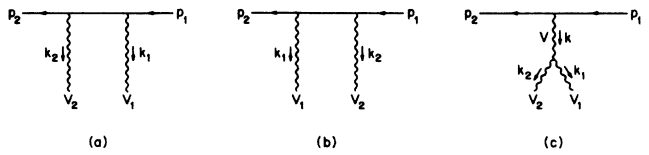

FIG. 1. Feynman diagrams for the $V_1V_2q_1q_2$ process. For $V_1V_2=\gamma\gamma, ZZ, Z\gamma$ diagram (c) does not contribute.

$$\Gamma^V(k_1,k_2)_\mu \equiv [e_1\cdot e_2(k_1-k_2)^\nu + 2k_2\cdot e_1 e_2^\nu - 2k_1\cdot e_2 e_1^\nu] \times \frac{g_{\mu\nu}+(\xi-1)k_\mu k_\nu/(k^2-\xi M_V^2)}{k^2-M_V^2+iM_V\Gamma_V(k^2)} , \quad (2.3)$$

where k_1 (k_2) and e_1 (e_2) are the four-momentum and polarization vector of the outgoing gauge boson V_1 (V_2) with $k=k_1+k_2$ and $\xi=1$, 0, or ∞ for the Feynman, Landau, or unitary gauge, respectively. $\Gamma_V(k^2)$ denotes an effective k^2-dependent width of V, which may be approximated by

$$\Gamma_V(k^2)=\Gamma_V\theta(k^2)k^2/M_V^2 \quad (2.4)$$

[θ is the step function, $\theta(x>0)=1$, $\theta(x<0)=0$]. Since we are treating all fermions as massless, no Goldstone-boson-exchange graphs enter when using other gauges than the unitary gauge for virtual weak bosons. Hence the Feynman gauge is the most economic gauge for all virtual gauge bosons. Using the bra and ket notation of Appendix A, it is easy to write a compact expression for the $V_1V_2q_{i_1}q_{i_2}$ amplitude:

$$\mathcal{M}=\delta_{i_1i_2}\{-F_{21}\langle 2|(\not\epsilon_2)_{\sigma_1}|k_1,1\rangle - F_{12}\langle 2|(\not\epsilon_1)_{\sigma_1}|k_2,1\rangle + F_0\langle 2|[\not V(k_1,k_2)]_{\sigma_1}|1\rangle\} . \quad (2.5)$$

Here $(\not\epsilon_i)_\pm$ denotes the contraction of the polarization vector e_i^μ of the electroweak boson V_i with the four Pauli matrices $(\sigma_\mu)_\pm$, and $\delta_{i_1i_2}$ is the color tensor (i_1 and i_2 are quark color indices). The relative signs of the amplitudes are due to the different signs for fermion and boson propagators. The normalization factors are given in terms of the electroweak coupling constants $g_{\sigma_i}^{Vf_if_j}$ defined in Appendix A [see Eq. (A19)], namely,

$$F_{21}=F_0\sum_f g_{\sigma_2}^{V_2f_2f}g_{\sigma_1}^{V_1ff_1} ,$$
$$F_{12}=F_0\sum_f g_{\sigma_2}^{V_1f_2f}g_{\sigma_1}^{V_2ff_1} , \quad (2.6)$$
$$F_0=S_1S_2\delta_{\sigma_1\sigma_2}(4\bar p_1^0\bar p_2^0)^{1/2} .$$

The $\sum_f$ runs over all contributing quark flavors when Cabibbo mixing is included. The last term in Eq. (2.5) describes the effect of the triple-weak-boson vertex. Interference effects between photon and Z exchange in the case of W^+W^- production are included by summing the four-vector $\Gamma^V(k_1,k_2)_\mu$ over the contributing virtual gauge bosons and weighting with the product of V fermion and VV_1V_2 couplings, i.e., the four-vector $\Gamma(k_1,k_2)_\mu$ in Eq. (2.5) is given by

$$\Gamma(k_1,k_2)_\mu=\sum_V g_{VV_1V_2}g_{\sigma_1}^{Vf_2f_2}\Gamma^V(k_1,k_2)_\mu , \quad (2.7)$$

where the nonvanishing $V\to V_1V_2$ three-vector-boson couplings are given by

$$g_{VW^-W^+}=g_{W^-VW^-}=g_{W^+W^+V}e \text{ for } V=\gamma , -g_{VW^+W^-}=-g_{W^+VW^+}=-g_{W^-W^-V}=\begin{cases} e & \text{for } V=\gamma, \\ e\cot\theta_W & \text{for } V=Z . \end{cases} \quad (2.8)$$

Thus the triple-vertex term [the last term in Eq. (2.5)] vanishes identically for $\gamma\gamma$, $Z\gamma$, and ZZ production. Similarly $F_{12}=0$ ($F_{21}=0$) for W^+W^- production from $u\bar u$ ($d\bar d$) annihilation, whereas all three terms in Eq. (2.6) contribute for $W^\pm\gamma$ and $W^\pm Z$ production.

B. *VVqqg*

Weak-boson pair production in association with one jet is calculated from the $VVqqg$ processes shown in Fig. 2. We denote the gluon polarization vector by ϵ^μ. The $V_1V_2q_{i_1}q_{i_2}g^a$ amplitude (a denotes the gluon color index, $a=1,\ldots,8$) is then given by

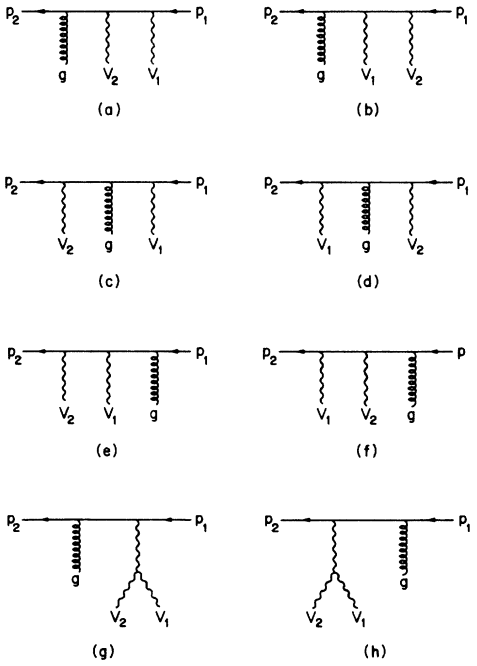

FIG. 2. Feynman diagrams for the $V_1V_2q_1q_2g$ process. For $V_1V_2=\gamma\gamma, ZZ, Z\gamma$ diagrams (g) and (h) do not contribute.

$$\mathcal{M}=g_s\left[\frac{\lambda^a}{2}\right]_{i_2 i_1}\{-F_{21}\langle 2,g|(\not\epsilon_2)_{\sigma_1}|k_1,1\rangle-F_{12}\langle 2,g|(\not\epsilon_1)_{\sigma_1}|k_2,1\rangle-F_{21}\langle 2,k_2|(\not\epsilon)_{\sigma_1}|k_1,1\rangle-F_{12}\langle 2,k_1|(\not\epsilon)_{\sigma_1}|k_2,1\rangle$$
$$-F_{21}\langle 2,k_2|(\not\epsilon_1)_{\sigma_1}|g,1\rangle-F_{12}\langle 2,k_1|(\not\epsilon_2)_{\sigma_1}|g,1\rangle$$
$$+F_0\langle 2,g|[\not\Gamma(k_1,k_2)]_{\sigma_1}|1\rangle+F_0\langle 2|[\not\Gamma(k_1,k_2)]_{\sigma_1}|g,1\rangle\}\ , \tag{2.9}$$

where F_{21}, F_{12}, and F_0 are given by the respective expressions in Eq. (2.6), and the additional factor of the strong coupling constant g_s is given explicitly in Eq. (2.9). The eight terms in Eq. (2.9) correspond to the eight diagrams in Fig. 2. For $\gamma\gamma$, $Z\gamma$, and ZZ production the triple-vertex terms [the last two terms in Eq. (2.9)] vanish identically and for W^+W^- production either $F_{12}=0$ or $F_{21}=0$.

C. *VVqqqq*

The *VVqqqq* subprocess is one of two subprocesses that contributes to weak-boson pair production in association with two jets (see Fig. 3). We start with the simple case of the $WVq_{i_1}q_{i_2}q_{i_3}q_{i_4}$ amplitude where $V=\gamma$ or Z and the flavors of the two incoming quarks 1 and 3 as well as of the two outgoing quarks 2 and 4 are different. Fixing the flavors of the external quarks, the W can only couple to one of the two quark lines, which we have chosen to be the q_1q_2 line in Fig. 3. The resulting amplitude can be written as

$$\mathcal{M}=\frac{\lambda^a_{i_2 i_1}}{2}\frac{\lambda^a_{i_4 i_3}}{2}\sum_{n=1}^{4}A_n\ , \tag{2.10}$$

where the four amplitudes

$$A_n=A_n(\bar p_1\bar\sigma_1 f_1,\bar p_2\bar\sigma_2 f_2,\bar p_3\bar\sigma_3 f_3,\bar p_4\bar\sigma_4 f_4)$$
$$\equiv A_n(1,2,3,4) \tag{2.11}$$

correspond to the four rows of Feynman graphs in Fig. 3:

$$A_1(1,2,3,4)=-C_1[\langle 2|(J_{43})_{\sigma_1}|\Gamma(k_1,k_2),1\rangle$$
$$+\langle 2,\Gamma(k_1,k_2)|(J_{43})_{\sigma_1}|1\rangle]\ ,$$
$$A_2(1,2,3,4)=C_{21}[\langle 2|(J_{43})_{\sigma_1}|k_2,k_1,1\rangle$$
$$+\langle 2,k_2,k_1|(J_{43})_{\sigma_1}|1\rangle$$
$$+\langle 2,k_2|(J_{43})_{\sigma_1}|k_1,1\rangle]\ ,$$
$$A_3(1,2,3,4)=C_{12}[\langle 2|(J_{43})_{\sigma_1}|k_1,k_2,1\rangle$$
$$+\langle 2,k_1,k_2|(J_{43})_{\sigma_1}|1\rangle$$
$$+\langle 2,k_1|(J_{43})_{\sigma_1}|k_2,1\rangle]\ , \tag{2.12}$$
$$A_4(1,2,3,4)=C_{24}[\langle 2|(\sigma^\lambda)_{\sigma_1}|k_1,1\rangle+\langle 2,k_1|(\sigma^\lambda)_{\sigma_1}|1\rangle]$$
$$\times[\langle 4|(\sigma_\lambda)_{\sigma_3}|k_2,3\rangle$$
$$+\langle 4,k_2|(\sigma_\lambda)_{\sigma_3}|3\rangle]\frac{1}{(p_1-p_2-k_1)^2}\ .$$

A_1 represents diagrams with a triple-gauge-boson coupling, A_2 and A_3 describe the emission of two gauge bosons from a single fermion line, and A_4 corresponds to emission of one gauge boson from each of the two quark lines. The coefficients C_i contain the overall normalization factor

$$C_0=g_s^2S_1S_2S_3S_4\delta_{\sigma_1\sigma_2}\delta_{\sigma_3\sigma_4}(16\bar p_1^0\bar p_2^0\bar p_3^0\bar p_4^0)^{1/2} \tag{2.13}$$

and the electroweak coupling constants

$$C_1=C_0\delta_{f_3f_4}\ ,$$
$$C_{21}=C_0\sum_f g_{\sigma_2}^{V_2f_2f}g_{\sigma_1}^{V_1ff_1}\delta_{f_3f_4}\ ,$$
$$C_{12}=C_0\sum_f g_{\sigma_2}^{V_1f_2f}g_{\sigma_1}^{V_2ff_1}\delta_{f_3f_4}\ , \tag{2.14}$$
$$C_{24}=C_0g_{\sigma_1}^{V_1f_2f_1}g_{\sigma_2}^{V_2f_4f_3}\ .$$

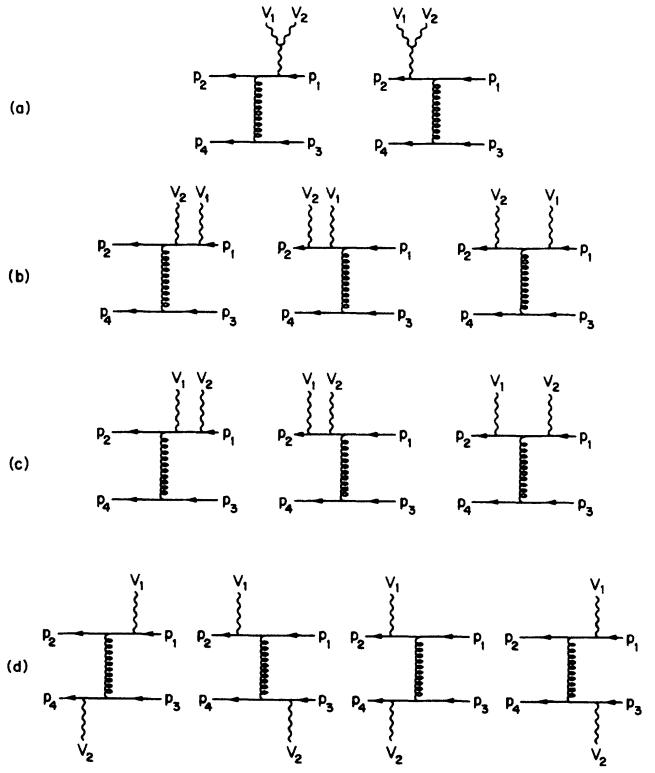

FIG. 3. Feynman diagrams for the $V_1V_2q_1q_2q_3q_4$ process. For $V_1V_2=\gamma\gamma,ZZ,Z\gamma$ diagrams (a) do not contribute. Diagrams obtained by interchanging the quark lines (1,2)↔(3,4) are not shown.

J^{μ}_{43} is the quark current corresponding to the lower parts of the Feynman diagrams in the first three rows of Fig. 3:

$$J^{\mu}_{43}=\langle 4|(\sigma^{\mu})_{\sigma_3}|3\rangle\frac{1}{(p_4-p_3)^2}\ . \tag{2.15}$$

In the case at hand only the color factor

$$T^{(1)}=\frac{\lambda^a_{i_2 i_1}}{2}\frac{\lambda^a_{i_4 i_3}}{2} \tag{2.16}$$

appears. Nevertheless it is useful for later generalization to the identical flavor case to expand $\mathcal{M}$ in terms of the orthogonal color tensors

$$\mathcal{O}^{\pm}=\frac{1}{2}\left[\frac{\lambda^a_{i_2 i_1}}{2}\frac{\lambda^a_{i_4 i_3}}{2}\pm\frac{\lambda^a_{i_2 i_3}}{2}\frac{\lambda^a_{i_4 i_1}}{2}\right]; \tag{2.17}$$

i.e., we write

$$\mathcal{M}=\sum_{m=\pm}\mathcal{M}^{(m)}\mathcal{O}^{(m)} \tag{2.18}$$

with

$$\mathcal{M}^{(+)}=\mathcal{M}^{(-)}=\sum_{n=1}^{4}A_n(1,2,3,4)\ . \tag{2.19}$$

When either the two incoming quarks (or the two outgoing quarks) have the same flavor, $f_1=f_3$ (or $f_2=f_4$), the complete amplitude has to be antisymmetrized in momentum and color indices. Since $\mathcal{O}^{(+)}$ ($\mathcal{O}^{(-)}$) is symmetric (antisymmetric) in color, the coefficients are

$$\mathcal{M}^{(\pm)}=\sum_{n=1}^{4}[A_n(1,2,3,4)\mp A_n(3,2,1,4)] \tag{2.20}$$

for $f_1=f_3$ and

$$\mathcal{M}^{(\pm)}=\sum_{n=1}^{4}[A_n(1,2,3,4)\mp A_n(1,4,3,2)] \tag{2.21}$$

for $f_2=f_4$.

For the general $V_1V_2q_{i_1}q_{i_2}q_{i_3}q_{i_4}$ amplitudes the contributing Feynman graphs are those shown in Fig. 3, as well as the ones obtained by interchanging the quark lines. This interchange of quark lines is easily taken into account by adding the amplitudes A_n with (1,2)↔(3,4) interchanged. Thus one obtains

$$\mathcal{M}^{(\pm)}=\sum_{n=1}^{4}[A_n(1,2,3,4)+A_n(3,4,1,2)] \tag{2.22}$$

for $f_1\neq f_3$ and $f_2\neq f_4$, while in the case of identical flavors ($f_1=f_3$ and/or $f_2=f_4$) the amplitudes need to be antisymmetrized with respect to identical fermions:

$$\mathcal{M}^{(\pm)}=\sum_{n=1}^{4}[A_n(1,2,3,4)\mp A_n(3,2,1,4)+A_n(3,4,1,2)\mp A_n(1,4,3,2)]\ . \tag{2.23}$$

Equation (2.23) holds for any combination of electroweak bosons and quarks when the restrictions on quark flavors are taken into account, which are made explicit in terms of Kronecker δ's in the coefficients C_i of Eq. (2.14) or which are implicit in the electroweak coupling constants $g^{Vf_if_j}_{\sigma_i}$ appearing in the C_i's and in $\Gamma(k_1,k_2)^{\mu}$ of Eq. (2.7).

When considering particular channels, these flavor restrictions simplify the resulting expressions considerably. For the $V_1V_2=\gamma\gamma,Z\gamma,ZZ$ amplitudes, the diagrams containing the triple-boson vertex do not contribute, i.e., $A_1\equiv 0$. For W^+W^+ or W^-W^- production only A_4 can contribute (emission of one W from each of the two quark lines) and the same is true for W^+W^- production when the flavors of, e.g., quarks 1 and 2 are different. For W^+W^- production with $f_1=f_2$ and $f_3=f_4$, on the other hand, $A_4=0$ and either A_2 or A_3 vanishes, while both photon and Z exchange contribute to the triple-gauge-boson vertex graphs which are summed into A_1. For the WV amplitudes ($V=\gamma,Z$) that we considered first one finds that Eqs. (2.22) and (2.23) reduce to Eqs. (2.20) and (2.21) due to the flavor restrictions.

D. *VVqqgg*

The *VVqqgg* subprocess is the other subprocess that contributes to *VV* plus two-jet production (see Fig. 4). The triple-gluon vertex ($g\to g_1g_2$) is introduced through a four-vector similar to the one for the triple-weak-boson vertex; we define

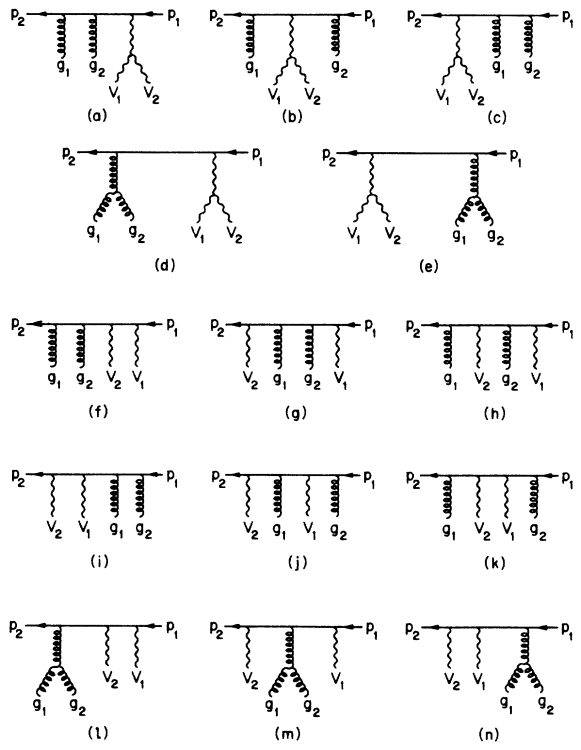

FIG. 4. Feynman diagrams for the $V_1V_2q_1q_2g_1g_2$ process. For $V_1V_2=\gamma\gamma,ZZ,Z\gamma$ diagrams (a)–(e) do not contribute. Diagrams obtained by interchanging $g_1\leftrightarrow g_2$ in diagrams (a)–(k) and $V_1\leftrightarrow V_2$ in diagrams (f)–(n) are not shown.

$$\Gamma^g(g_1,g_2)^\mu \equiv [\epsilon_1\cdot\epsilon_2(g_1-g_2)^\mu + 2g_2\cdot\epsilon_1\epsilon_2^\mu - 2g_1\cdot\epsilon_2\epsilon_1^\mu]\frac{1}{(g_1+g_2)^2}\ , \tag{2.24}$$

where we have chosen the Feynman gauge for the virtual gluon.

For the $V_1V_2q_{i_1}q_{i_2}g^{a_1}g^{a_2}$ process it is convenient to define the coefficients B_n of the color tensor

$$T^{(1)} = \left[\frac{\lambda^{a_1}}{2}\frac{\lambda^{a_2}}{2}\right]_{i_2 i_1}$$

as the basic quantities. The terms in the amplitudes $B_n(1,2)=B_n(\bar{g}_1\bar{\kappa}_1,\bar{g}_2\bar{\kappa}_2)$ are written here in the same order as the corresponding diagrams appear in Fig. 4:

$$B_1(1,2)=g_s^2F_0\{\langle 2,g_1,g_2|[\mathcal{V}(k_1,k_2)]_{\sigma_1}|1\rangle+\langle 2,g_1|[\mathcal{V}(k_1,k_2)]_{\sigma_1}|g_2,1\rangle$$
$$+\langle 2|[\mathcal{V}(k_1,k_2)]_{\sigma_1}|g_1,g_2,1\rangle-\langle 2,\Gamma^g(g_1,g_2)|[\mathcal{V}(k_1k_2)]_{\sigma_1}|1\rangle-\langle 2|[\mathcal{V}(k_1,k_2)]_{\sigma_1}|\Gamma^g(g_1,g_2),1\rangle\}\ ,$$

$$B_2(1,2)=g_s^2F_{21}\{-\langle 2,g_1,g_2|(\not\epsilon_2)_{\sigma_1}|k_1,1\rangle-\langle 2,k_2,g_1|(\not\epsilon_2)_{\sigma_1}|k_1,1\rangle$$
$$-\langle 2,g_1,k_2|(\not\epsilon_2)_{\sigma_1}|k_1,1\rangle-\langle 2,k_2,k_1|(\not\epsilon_1)_{\sigma_1}|g_2,1\rangle-\langle 2,k_2,g_1|(\not\epsilon_1)_{\sigma_1}|g_2,1\rangle-\langle 2,g_1,k_2|(\not\epsilon_1)_{\sigma_1}|g_2,1\rangle$$
$$+\langle 2|[\mathcal{V}^g(g_1,g_2)]_{\sigma_1}|k_2,k_1,1\rangle+\langle 2,k_2|[\mathcal{V}^g(g_1,g_2)]_{\sigma_1}|k_1,1\rangle+\langle 2,k_2,k_1|[\mathcal{V}^g(g_1,g_2)]_{\sigma_1}|1\rangle\}\ , \tag{2.25}$$

$$B_3(1,2)=g_s^2F_{12}[-\langle 2,g_1,g_2|(\not\epsilon_1)_{\sigma_1}|k_2,1\rangle-\langle 2,k_1,g_1|(\not\epsilon_2)_{\sigma_1}|k_2,1\rangle$$
$$-\langle 2,g_1,k_1|(\not\epsilon_2)_{\sigma_1}|k_2,1\rangle-\langle 2,k_1,k_2|(\not\epsilon_1)_{\sigma_1}|g_2,1\rangle-\langle 2,k_1,g_1|(\not\epsilon_2)_{\sigma_1}|g_2,1\rangle-\langle 2,g_1,k_1|(\not\epsilon_2)_{\sigma_1}|g_2,1\rangle$$
$$+\langle 2|[\mathcal{V}^g(g_1,g_2)]_{\sigma_1}|k_1,k_2,1\rangle+\langle 2,k_1|[\mathcal{V}^g(g_1,g_2)]_{\sigma_1}|k_2,1\rangle+\langle 2,k_1,k_2|[\mathcal{V}^g(g_1,g_2)]_{\sigma_1}|1\rangle]\ .$$

Here F_0, F_{21}, and F_{12} are given by the respective expressions in Eq. (2.6). Symmetrizing the amplitudes in the two gluons, the complete amplitude is

$$\mathcal{M}=\sum_{n=1}^{3}\{[B_n(1,2)+B_n(2,1)]\mathcal{O}^{(+)}+[B_n(1,2)-B_n(2,1)]\mathcal{O}^{(-)}\}\ ,$$
$$=\mathcal{M}^{(+)}\mathcal{O}^{(+)}+\mathcal{M}^{(-)}\mathcal{O}^{(-)}\ , \tag{2.26}$$

where the orthogonal color basis $\mathcal{O}^{(\pm)}$ is defined in Eqs. (B5) and (B6). For $\gamma\gamma$, $Z\gamma$, and ZZ production, the sum should start at $n=2$ since there is no contributing diagram with a triple-weak-boson vertex in these cases.

E. Off-shell weak bosons

The amplitudes in the previous sections were written for on-shell vector bosons, for which the polarization vectors, $e^\mu(\bar{k},\bar{\lambda})$ for electroweak vector bosons and $\epsilon^\mu(\bar{g},\bar{\kappa})$ for gluons, can be calculated directly from the momentum vectors $\bar{k}$ and $\bar{g}$ (see Appendix A). The corresponding amplitudes for virtual weak bosons decaying into fermions are obtained by replacing the polarization vectors e_l^μ with the decay currents. This replacement is indicated in Fig. 5. The additional elements of the Feynman graph including V decay are the V propagator factor and the lepton current describing the decay process $V\to\bar{l}_1\bar{l}_2$. In our two-component Weyl-spinor notation the effective replacement hence is

$$e^\mu\to j^\mu=-g_{\rho_1}^{Vl_2l_1}D_V(k^2)s_1s_2\delta_{\rho_1\rho_2}\times(4\bar{l}_1^0\bar{l}_2^0)^{1/2}\chi^\dagger_{\rho_2}(\bar{l}_2)(\sigma^\mu)_{\rho_1}\chi_{\rho_1}(\bar{l}_1)$$
$$=-g_{\rho_1}^{Vl_2l_1}D_V(k^2)s_1s_2\delta_{\rho_1\rho_2}\times(4\bar{l}_1^0\bar{l}_2^0)^{1/2}\langle l_2|(\sigma^\mu)_{\rho_1}|l_1\rangle\ . \tag{2.27}$$

Here s_1 and s_2 are the sign factors relating the physical momenta $\bar{l}_1$ and $\bar{l}_2$ to l_1 and l_2, i.e., $s_1=-,s_2=+$ in the decay process, and $\bar{\rho}_1=s_1\rho_1$ and $\bar{\rho}_2=s_2\rho_2$ describe the physical helicities of the V decay leptons. The V propagator factor $D_V(k^2)$ is written in terms of the momentum

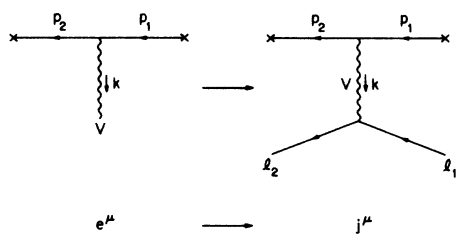

FIG. 5. Feynman rule for replacing the polarization vector of a real gauge boson with the production or decay current; see Eq. (2.27).

$k = l_2 - l_1 = s_2\bar{l}_2 - s_1\bar{l}_1$, and it is given by

$$D_V(k^2) = [k^2 - M_V^2 + iM_V\Gamma_V(k^2)]^{-1} . \tag{2.28}$$

The sign factors s_i are needed when using the amplitudes for crossing related processes, e.g., Eq. (2.27) with $s_1 = s_2 = +$ describes the virtual electroweak boson in $e^- p$ scattering.

For V_1V_2 production (in association with $n = 0,1,2$ jets) the full amplitudes, including the decays of V_1 and V_2 into final-state leptons, are obtained by replacing the polarization vectors of both virtual bosons by the respective decay currents

$$\begin{aligned} e_1^\mu \to j_1^\mu &= -g_{\rho_1}^{V_1 l_2 l_1} D_{V_1}(k_1^2) s_1 s_2 \delta_{\rho_1\rho_2} \\ &\quad \times (4\bar{l}_1^0 \bar{l}_2^0)^{1/2} \langle l_2 | (\sigma^\mu)_{\rho_1} | l_1 \rangle , \\ e_2^\nu \to j_2^\nu &= -g_{\rho_3}^{V_2 l_4 l_3} D_{V_2}(k_2^2) s_3 s_4 \delta_{\rho_3\rho_4} \\ &\quad \times (4\bar{l}_3^0 \bar{l}_4^0)^{1/2} \langle l_4 | (\sigma^\mu)_{\rho_3} | l_3 \rangle . \end{aligned} \tag{2.29}$$

For neutral currents the full amplitudes should be summed over $V = \gamma$ and Z exchanges.

III. APPLICATION

We have applied the formalism of the previous section to calculate the cross sections for $V_1V_2 + n$-jet ($n = 0,1,2$) production in $\bar{p}p$ collisions at $\sqrt{s} = 1.8$ TeV and in pp collisions at $\sqrt{s} = 17$ and 40 TeV. At the outset we checked that the parton-level cross sections are independent of the gauge parameter ξ and that they are invariant under Lorentz boosts. Since our amplitude expressions lack *manifest* Lorentz invariance these two tests are very powerful checks of the correctness of our computer programs. Folding the parton cross sections with the structure functions of the incoming hadrons, we reproduced previous calculations of $p\bar{p} \to V_1V_2$ production with zero[1,2,4] and one jet.[14]

In the following we use the SM parameters $M_Z = 91.1$ GeV, $M_W = 80.0$ GeV, and $\alpha(M_W) = 1/128$. These mass values are consistent with recent measurements at the Tevatron,[23] the SLAC Linear Collider,[24] and the CERN e^+e^- collider LEP (Ref. 25). The QCD running coupling constant is evaluated in lowest order with five active flavors. The scale Λ is taken to be 200 MeV for four flavors. The Q^2 scale of $\alpha_s(Q^2)$ is taken to be the squared average p_T of the outgoing particles: $Q^2 = [(1/n)\sum p_T]^2$. Uncertainties in the cross-section predictions associated with the Q^2 choice will be similar to those recently discussed for $W,Z + n$-jet production in Ref. 8. The choice of $Q^2 = \hat{s}$ gives the smallest cross sections, while other choices can increase the $VV + 2$-jet cross sections by up to a factor of 2. We have chosen the parton distribution functions of Eichten-Hinchliffe-Lane-Quigg (EHLQ) set I (Ref. 2), with $Q^2 = \hat{s}$.

To make an approximate detector simulation we impose the following acceptance requirements on the transverse momenta p_T, rapidities y, and pair separations $\Delta R = [(\Delta\phi)^2 + (\Delta y)^2]^{1/2}$ at $\sqrt{s} = 1.8$ (17 or 40) TeV:

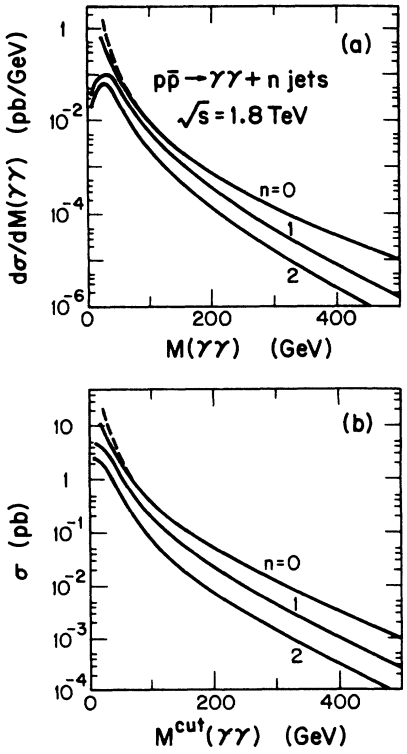

FIG. 6. Cross section for $p\bar{p} \to \gamma\gamma + n$-jet production at $\sqrt{s} = 1.8$ TeV: (a) as a function of the $\gamma\gamma$ invariant mass $M(\gamma\gamma)$; (b) cross section integrated above a minimum $M(\gamma\gamma)$.

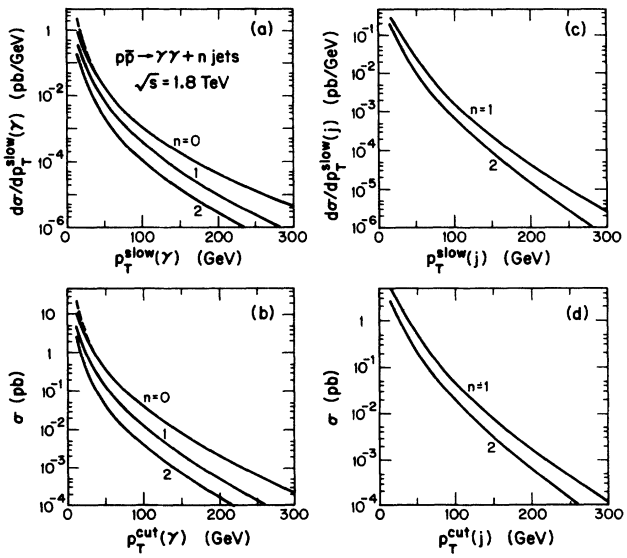

FIG. 7. Cross section for $p\bar{p} \to \gamma\gamma + n$-jet production at $\sqrt{s} = 1.8$ TeV: (a) as a function of the smaller of the transverse momenta of the two photons; (b) cross section integrated above a minimum $p_T(\gamma)$; (c) as a function of the smallest jet p_T; (d) integrated cross section above a minimum $p_T(j)$.

TABLE I. Predicted cross section (in pb) for $p\bar{p} \to VV + n$ jets at the Tevatron. Kinematical cuts imposed in the calculations are $|y(\gamma)| < 1$; $|y(W,Z)| < 2.5$; $|y(j)| < 2.5$; $p_T(\gamma) > 10$ GeV; $p_T(j) > 15$ GeV; $\Delta R_{\gamma j} > 0.7$; $\Delta R_{jj} > 0.7$.

$\sqrt{s} = 1.8$ TeV	$n=0$	$n=1$	$n=2$
$\gamma\gamma$	11	5	2.4
$\gamma W^+ + \gamma W^-$	5.4	2.7	0.9
γZ	7	2	0.5
W^+W^-	6.7	2.3	0.5
$ZW^+ + ZW^-$	1.7	0.6	0.2
ZZ	0.7	0.3	0.05

$$p_T(\gamma) > 10\ (25)\ \text{GeV},\quad p_T(j) > 15\ (100)\ \text{GeV},$$
$$|y(\gamma)| < 1.0\ (2.5),\quad |y(W,Z)| < 2.5\ (2.5), \tag{3.1}$$
$$|y(j)| < 2.5\ (2.5),\quad \Delta R_{\gamma j} > 0.7,\quad \Delta R_{jj} > 0.7,$$

where j denotes a jet. The predicted $V_1V_2 + n$-jet cross sections for these cuts are given in Tables I–III for Tevatron, LHC, and SSC energies. At supercollider energies the rate from $t\bar{t} \to WWb\bar{b}$ may be expected to dominate the $WW + n$-jet electroweak processes. The latter process cannot be reliably calculated until the top-quark mass is known; consequently its contribution is not included in the tables.

The results in Tables I–III are mainly for illustration, since for particular applications different choices of acceptance cuts may be required. Nevertheless a few remarks are appropriate about the cross-section predictions. The cross sections for $n = 1$ and 2 jets are substantial in comparison to the 0-jet rate. This enhancement of the $n = 1,2$ jet rate is due in part to the appearance of channels (gq and gg in the initial state) which are not present for $n = 0$. In addition, the radiation amplitude zero[26] in the $W\gamma$ case gives a suppression of the $n = 0$ cross section, explaining the fact that γZ and γW production have comparable cross sections for the zero-jet case. (Naively one would expect a larger $W\gamma$ rate due to the larger coupling of W's to the quarks.)

At the Tevatron energy the $\gamma\gamma$ channel gives the largest signal, with a cross section that can be measured. With the current luminosity of 4.7 pb^{-1} and the cuts in Eq. (3.1), we expect about 50, 20, and 10 $\gamma\gamma$ events with $n_j = 0, 1, 2$. For an eventual luminosity of 100 pb^{-1}, there would be 1000, 400, 200 events with $n_j = 0,1,2$. The

TABLE II. Predicted cross sections (in pb) for $pp \to VV + n$ jets at the LHC. Kinematical cuts imposed in the calculations are $|y(V)| < 2.5$; $|y(j)| < 2.5$; $p_T(\gamma) > 25$ GeV; $p_T(j) > 100$ GeV; $\Delta R_{\gamma j} > 0.7$; $\Delta R_{jj} > 0.7$.

$\sqrt{s} = 17$ TeV	$n=0$	$n=1$	$n=2$
$\gamma\gamma$	18	2	1.1
$\gamma W^+ + \gamma W^-$	19	11	2.8
γZ	18	2	0.7
W^+W^-	50	10	2.4
$ZW^+ + ZW^-$	18	8	2
ZZ	7.8	0.9	0.2

TABLE III. Same as Table II, but at $\sqrt{s} = 40$ TeV (SSC).

$\sqrt{s} = 40$ TeV	$n=0$	$n=1$	$n=2$
$\gamma\gamma$	32	5.3	4
$\gamma W^+ + \gamma W^-$	37	35	11
γZ	33	5.7	2.4
W^+W^-	101	33	10
$ZW^+ + ZW^-$	38	27	8.3
ZZ	17	3.1	1.1

$M(\gamma\gamma)$ invariant-mass distributions are shown in Fig. 6. The dashed curve in the $n = 0$ case includes the contribution from the $gg \to \gamma\gamma$ loop diagram[27] which enhances the $\gamma\gamma$ cross section by a factor of about 2 for $M(\gamma\gamma) < 50$ GeV. Similar enhancements at low gauge-boson pair invariant mass are present for $gg \to WW, ZZ$ at supercollider energies.[28] Figure 7 gives the dependence of the $\gamma\gamma$ cross section on the lowest photon p_T and the lowest jet p_T. Note that the cross sections decrease steeply as the γ and jet p_T-acceptance cuts are raised.

A more detailed discussion of the relevance of these pertubative-QCD calculations for physics at pp supercollider energies will be presented elsewhere.[29]

ACKNOWLEDGMENTS

We thank U. Baur for comparing the results from Ref. 14 with our calculations. This research was supported in part by the University of Wisconsin Research Committee with funds granted by the Wisconsin Alumni Research Foundation, and in part by the U.S. Department of Energy under Contract No. DE-AC02-76ER00881.

APPENDIX A

In this appendix we explain the shorthand notation used in the text and we explain how external spinors and vector-boson polarization vectors are obtained from the momenta of the external particles in an arbitrary Lorentz frame. The resulting expressions can be directly used in a numerical program.

The helicity-amplitude formalism developed in Ref. 22 is used to handle the Dirac algebra. We start with a brief review of the spinor calculus. By using the chiral representation of Dirac matrices for all fermions, two-component notation becomes very convenient. Four-component Dirac spinors $\psi(\bar{p},\bar{\sigma})$[$= u(\bar{p},\bar{\sigma})$ or $v(\bar{p},\bar{\sigma})$] are then expressed by two two-component Weyl spinors $\psi_{\pm}$:

$$\psi = \begin{bmatrix} \psi_- \\ \psi_+ \end{bmatrix},\quad \bar{\psi} = (\psi_+^{\dagger}, \psi_-^{\dagger}), \tag{A1}$$

with

$$u(\bar{p},\bar{\sigma})_{\pm} = \omega_{\pm\bar{\sigma}}(\bar{p})\chi_{\bar{\sigma}}(\bar{p}),$$
$$v(\bar{p},\bar{\sigma})_{\pm} = \pm\bar{\sigma}\omega_{\mp\bar{\sigma}}(\bar{p})\chi_{-\bar{\sigma}}(\bar{p}). \tag{A2}$$

Here $\bar{\sigma}$ denotes the helicity of the on-shell fermion with

four-momentum $\bar{p}^\mu=(\bar{E},\bar{p}_x,\bar{p}_y,\bar{p}_z)$, $\chi_{\bar{\sigma}}(\bar{p})$ is a normalized helicity eigenspinor explicitly given by

$$\chi_+(\bar{p})=[2|\bar{\mathbf{p}}|(|\bar{\mathbf{p}}|+\bar{p}_z)]^{-1/2}\begin{bmatrix}|\bar{\mathbf{p}}|+\bar{p}_z\\ \bar{p}_x+i\bar{p}_y\end{bmatrix}, \tag{A3a}$$

$$\chi_-(\bar{p})=[2|\bar{\mathbf{p}}|(|\bar{\mathbf{p}}|+\bar{p}_z)]^{-1/2}\begin{bmatrix}-\bar{p}_x+i\bar{p}_y\\ |\bar{\mathbf{p}}|+\bar{p}_z\end{bmatrix}, \tag{A3b}$$

and

$$\omega_\pm(\bar{p})=(\bar{E}\pm|\bar{\mathbf{p}}|)^{1/2}. \tag{A4}$$

In the massless fermion limit $\omega_-(\bar{p})$ vanishes and the spinors (A2) simplify considerably. Using the sign factor S introduced in Eq. (2.1) ($S=+$ for fermions, $S=-$ for antifermions) both u and v spinors can be expressed as

$$\psi(\bar{p},\bar{\sigma})_\pm=S\delta_{\sigma,\pm}\sqrt{2\bar{E}}\,\chi_\sigma(\bar{p}) \tag{A5a}$$

with

$$\sigma=S\bar{\sigma} \tag{A5b}$$

which yields the simple crossing relations used throughout this paper.

The contraction of a four-vector a^μ with a γ matrix is given by

$$\not{a}=a^\mu\gamma_\mu=\begin{bmatrix}0 & (\not{a})_+\\ (\not{a})_- & 0\end{bmatrix}, \tag{A6}$$

where, explicitly,

$$(\not{a})_\pm=a_\mu\sigma^\mu_\pm=\begin{bmatrix}a^0\mp a^3 & \mp(a^1-ia^2)\\ \mp(a^1+ia^2) & a^0\pm a^3\end{bmatrix}. \tag{A7}$$

In a numerical program the sign factor S_i, the physical momentum $\bar{p}_i=S_ip_i$, and the physical helicity $\bar{\sigma}_i=S_i\sigma_i$ of any external (anti)fermion can be identified by a single integer i. Hence we use the bra-ket shorthand notation [see Fig. 8(a)]

$$\langle i|=\chi^\dagger_{\sigma_i}(\bar{p}_i),\quad |i\rangle=\chi_{\sigma_i}(\bar{p}_i). \tag{A8}$$

The emission of a vector boson with momentum k_1 and polarization vector e_1^μ, from the external fermion i [see Fig. 8(b)] is described by a unique complex two-vector which we denote by

$$\begin{aligned}\langle i,k_1|&=\chi^\dagger_{\sigma_i}(\bar{p}_i)(\not{e}_1)_{\sigma_1}\frac{(\not{p}_i+\not{k}_1)_{-\sigma_i}}{(p_i+k_1)^2},\\ |k_1,i\rangle&=\frac{(\not{p}_i-\not{k}_1)_{-\sigma_i}}{(p_i-k_1)^2}(\not{e}_1)_{\sigma_i}\chi_{\sigma_i}(\bar{p}_i).\end{aligned} \tag{A9}$$

Notice the different relative signs between p_i and k_1, due to the convention that boson momenta are chosen as outgoing whereas the fermion momentum is taken along the fermion number flow. Since for a given process a particular external fermion appears as either bra or ket, but never as both, no confusion will arise due to the fact that $\langle i,k_1|\neq|k_1,i\rangle^\dagger$ in Eq. (A9). In theories with fermion-number violation (e.g., with Majorana fermions), this shorthand notation should be used with extra care.

The emission of two vector bosons with momenta k_1,k_2 and polarization vectors e_1^μ,e_2^μ, from the external fermion i [see Fig. 8(c)] is also described by a unique complex two-vector which we denote by

$$\begin{aligned}\langle i,k_1,k_2|&=\chi^\dagger_{\sigma_i}(\bar{p}_i)(\not{e}_1)_{\sigma_i}\frac{(\not{p}_i+\not{k}_1)_{-\sigma_i}}{(p_2+k_1)^2}(\not{e}_2)_{\sigma_i}\\ &\quad\times\frac{(\not{p}_i+\not{k}_1+\not{k}_2)_{-\sigma_i}}{(p_i+k_1+k_2)^2},\\ |k_2,k_1,i\rangle&=\frac{(\not{p}_i-\not{k}_1-\not{k}_2)_{-\sigma_i}}{(p_i-k_1-k_2)^2}(\not{e}_2)_{\sigma_i}\\ &\quad\times\frac{(\not{p}_i-\not{k}_1)_{-\sigma_1}}{(p_i-k_1)^2}(\not{e}_1)_{\sigma_i}\chi_{\sigma_i}(\bar{p}_i).\end{aligned} \tag{A10}$$

Note the recursive relationship between the bra's and ket's in the last three equations:

$$\begin{aligned}\langle i,k_1,\ldots,k_n|&=\langle i,k_1,\ldots,k_{n-1}|(\not{e}_n)_{\sigma_i}\\ &\quad\times\frac{(\not{p}_i+\not{k}_1+\cdots+\not{k}_n)_{-\sigma_i}}{(p_i+k_1+\cdots+k_n)^2},\\ |k_n,\ldots,k_1,i\rangle&=\frac{(\not{p}_i-\not{k}_1-\cdots-\not{k}_n)_{-\sigma_i}}{(p_i-k_1-\cdots-k_n)^2}\\ &\quad\times(\not{e}_n)_{\sigma_i}|k_{n-1},\ldots,k_1,i\rangle.\end{aligned} \tag{A11}$$

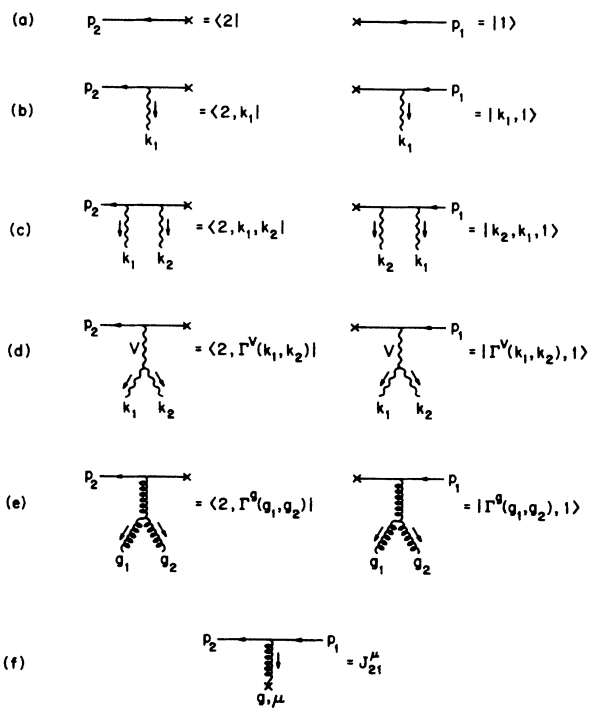

FIG. 8. Feynman rules for the abbreviations used in the text: See Eq. (A8) for (a), Eq. (A9) for (b), Eq. (A10) for (c), Eq. (A12) for (d), Eq. (A13) for (e), and Eq. (2.15) for (f).

This recursive relationship makes it especially easy to evaluate the bra's and ket's in a computer program; $\langle i|$ and $|i\rangle$ are evaluated first and are then used to evaluate $\langle i,k_1|$ and $|k_1,i\rangle$, which are in turn used to evaluate $\langle i,k_1,k_2|$ and $|k_2,k_1,i\rangle$.

The emission of two vector bosons via the triple-boson coupling can also be described by a unique complex two-vector which we denote by

$$\langle i,\Gamma^V(k_1,k_2)|=\chi^{\dagger}_{\sigma_i}(\bar{p}_i)[\not{V}^V(k_1,k_2)]_{\sigma_i}\frac{(\not{p}_i+\not{k}_1+\not{k}_2)_{-\sigma_i}}{(p_i+k_1+k_2)^2}\ , \tag{A12}$$

$$|\Gamma^V(k_1,k_2),i\rangle=\frac{(\not{p}_i-\not{k}_1-\not{k}_2)_{-\sigma_i}}{(p_i-k_1-k_2)^2}[\not{V}^V(k_1,k_2)]_{\sigma_i}\chi_{\sigma_i}(\bar{p}_i)\ .$$

Here k_1,k_2 are the momenta of the two external bosons, $\Gamma^V(k_1,k_2)$ is the four-vector defined in Eq. (2.3), and i is the external fermion [see Fig. 8(d)]. Similarly, we also introduce complex two-vectors associated with the emission of two gluons via the triple-gluon coupling [see Fig. 8(e)]:

$$|\Gamma^g(g_1,g_2),1\rangle=\frac{(\not{p}_1-\not{g}_1-\not{g}_2)_{-\sigma_1}}{(p_1-g_1-g_2)^2}[\not{V}^g(g_1,g_2)]_{\sigma_1}\chi_{\sigma_1}(\bar{p}_1)\ , \tag{A13}$$

$$\langle 2,\Gamma^g(g_1,g_2)|=\chi^{\dagger}_{\sigma_2}(\bar{p}_2)[\not{V}^g(g_1,g_2)]_{\sigma_2}\frac{(\not{p}_2+\not{g}_1+\not{g}_2)_{-\sigma_2}}{(p_2+g_1+g_2)^2}\ .$$

All of these abbreviations are summarized in Fig. 8.

In analogy to the spinors describing external fermions, vector-boson polarization vectors can also be obtained directly from the vector-boson momentum $\bar{k}^{\mu}$, in an arbitrary reference frame. With

$$\bar{k}^{\mu}=(\bar{E},\bar{k}_x,\bar{k}_y,\bar{k}_z),\quad \bar{E}=(|\bar{\mathbf{k}}|^2+m^2)^{1/2}\ ,$$
$$\bar{k}_T=(\bar{k}_x^2+\bar{k}_y^2)^{1/2}\ , \tag{A14}$$

we choose, as a rectangular polarization basis,

$$\bar{\epsilon}^{\mu}(\bar{k},\bar{\lambda}=1)=(|\bar{\mathbf{k}}|\bar{k}_T)^{-1}(0,\bar{k}_x\bar{k}_z,\bar{k}_y\bar{k}_z,-\bar{k}_T^2)\ , \tag{A15a}$$

$$\bar{\epsilon}^{\mu}(\bar{k},\bar{\lambda}=2)=(\bar{k}_T)^{-1}(0,-\bar{k}_y,\bar{k}_x,0)\ , \tag{A15b}$$

$$\bar{\epsilon}^{\mu}(\bar{k},\bar{\lambda}=3)=(\bar{E}/m|\bar{\mathbf{k}}|)(|\bar{\mathbf{k}}|^2/\bar{E},\bar{k}_x,\bar{k}_y,\bar{k}_z)\ . \tag{A15c}$$

The $\lambda=3$ polarization vector of (A15c) represents longitudinal polarization for a massive vector boson. For massless vector bosons only the $\lambda=1$ and 2 polarization states are physical.

Helicity eigenvectors are obtained from the above polarization vectors by forming the sum

$$\bar{\epsilon}^{\mu}(\bar{k},\bar{\lambda}=\pm)=\mp\frac{1}{\sqrt{2}}[\bar{\epsilon}^{\mu}(\bar{k},\bar{\lambda}=1)\pm i\bar{\epsilon}^{\mu}(\bar{k},\bar{\lambda}=2)]\ . \tag{A16}$$

The polarization vectors of the rectangular basis (A15) can be used for both incoming and outgoing vector bosons since all their components are real numbers.

Note that we ignore complex conjugation for outgoing vector-boson wave functions, $e^{\mu}(\bar{k},\bar{\lambda})$ for V and $\epsilon^{\mu}(\bar{g},\bar{\kappa})$ for gluons, throughout this paper. This is valid in the orthogonal basis ($\bar{\lambda}=1,2,3$, and $\bar{\kappa}=1,2$) that we choose as a standard basis since then their components are all real. For complex wave functions, e.g., in the helicity basis, one should introduce one more crossing notation for e^{μ} and ϵ^{μ} by defining the "physical" wave function $\bar{e}^{\mu}$ and $\bar{\epsilon}^{\mu}$. Since in our amplitudes all vector bosons are chosen outgoing by convention, one has the crossing relations

$$e^{\mu}(\bar{k},\bar{\lambda})=\bar{e}^{\mu}(\bar{k},\bar{\lambda})^*\ \text{ if } k=\bar{k}\ (S=+)\ ,$$
$$e^{\mu}(\bar{k},\bar{\lambda})=\bar{e}^{\mu}(\bar{k},\bar{\lambda})\ \text{ if } k=-\bar{k}\ (S=-)\ , \tag{A17}$$

and similarly for $\epsilon^{\mu}(\bar{g},\bar{\kappa})$. They are needed only when one measures polarizations of V's or gluons. When the V wave function e^{μ} is replaced by the decay current j^{μ} of Eq. (2.27), the crossing is taken care of by the relations for the fermion legs alone.

The helicity amplitudes also contain the electroweak coupling constants. The left- and right-handed coupling constants $g_{\sigma_i}^{Vf_if_j}$ are described by the V-fermion interaction Lagrangian

$$\mathcal{L}_{\text{int}}=-\sum_{\tau=\pm}g_{\tau}^{Vf_1f_2}\bar{\psi}_1\gamma^{\mu}\tfrac{1}{2}(1+\tau\gamma_5)\psi_2V_{\mu}\ . \tag{A18}$$

The relevant couplings in the standard model are

$$g_{\pm}^{\gamma ff}=eQ_f,\quad g_{+}^{Zff}=-eQ_f\tan\theta_W\ ,$$
$$g_{-}^{Zff}=eT_{3f}/(\sin\theta_W\cos\theta_W)-eQ_f\tan\theta_W\ ,$$
$$g_{-}^{We\nu}=g_{-}^{We\nu}=e/(\sqrt{2}\sin\theta_W)\ , \tag{A19}$$
$$g_{-}^{Wu_id_j}=(g_{-}^{Wd_ju_i})^*=eU_{ij}/(\sqrt{2}\sin\theta_W)\ ,$$

where Q_f and T_{3f} denote the electric charge (in units of the proton charge, e) and the weak isospin of the fermion f, θ_W is the weak mixing angle, and U_{ij} denotes the Cabibbo-Kobayashi-Maskawa matrix elements with the notation $(u_1,u_2,u_3)=(u,c,t)$ and $(d_1,d_2,d_3)=(d,s,b)$ for quark mass eigenstates.

APPENDIX B

In this appendix we describe the orthogonal color tensors used to write the $VVqqqq$ and $VVqqgg$ amplitudes. A complete discussion of orthogonal color tensors can be found in Ref. 30.

The amplitudes for the $VVqq$ and $VVqqg$ processes have a very simple structure in color space. Only one tensor (in color indices) appears, namely, $\delta_{i_2i_1}$ or $\frac{1}{2}\lambda^a_{i_2i_1}$. Hence, when performing the sum over colors in the calculation of cross-section formulas

$$d\sigma\sim\sum_{\text{colors}}|\mathcal{M}|^2\ , \tag{B1}$$

we merely get an overall factor of

$$\sum_{i_1,i_2}|\delta_{i_2i_1}|^2=\text{tr}\mathbf{1}=N \tag{B2}$$

for the $VVqq$ process and

$$\sum_{i_1,i_2,a}\left|\frac{\lambda^a_{i_2i_1}}{2}\right|^2=\text{tr}\frac{\lambda^a}{2}\frac{\lambda^a}{2}=(N^2-1)/2 \tag{B3}$$

for the $VVqqg$ process in an SU(N) gauge theory.

The $VVqqqq$ and $VVqqgg$ amplitudes are both linear combinations of two color tensors, namely,

$$T^{(1)}=\frac{\lambda^a_{i_2 i_1}}{2}\frac{\lambda^a_{i_4 i_3}}{2},\quad T^{(2)}=\frac{\lambda^a_{i_2 i_3}}{2}\frac{\lambda^a_{i_4 i_1}}{2}\ , \tag{B4}$$

for the $VVqqqq$ amplitude, and

$$T^{(1)}=\left[\frac{\lambda^{a_1}}{2}\frac{\lambda^{a_2}}{2}\right]_{i_2 i_1}\ ,$$
$$T^{(2)}=\left[\frac{\lambda^{a_2}}{2}\frac{\lambda^{a_1}}{2}\right]_{i_2 i_1}\ , \tag{B5}$$

for the $VVqqgg$ amplitude. In order to get compact expressions for the color-summed squared matrix elements it is more convenient to expand the Feynman amplitudes in terms of the symmetric and antisymmetric combinations

$$\mathcal{O}^{(\pm)}=\tfrac{1}{2}(T^{(1)}\pm T^{(2)})\ . \tag{B6}$$

The coefficients $\mathcal{M}^{(\pm)}$ of this expansion

$$\mathcal{M}=\sum_{m=\pm}\mathcal{M}^{(m)}\mathcal{O}^{(m)}\ , \tag{B7}$$

which contain the full momentum dependence of the amplitudes, have been given in Sec. II. Because of the different symmetry properties of $\mathcal{O}^{(+)}$ and $\mathcal{O}^{(-)}$ no cross terms occur in the amplitude squared and one obtains, for the color sum,

$$\sum_{\text{colors}}|\mathcal{M}|^2=\sum_{m=\pm}c_m|\mathcal{M}^{(m)}|^2 \tag{B8}$$

with simple numeric coefficients c_m.

More explicitly, for the color group SU(3), one finds, for the $VVqqqq$ process,

$$\sum_{\text{colors}}|\mathcal{M}|^2=\tfrac{2}{3}|\mathcal{M}^{(+)}|^2+\tfrac{4}{3}|\mathcal{M}^{(-)}|^2\ , \tag{B9}$$

while the result for the $VVqqgg$ cross sections is given by

$$\sum_{\text{colors}}|\mathcal{M}|^2=\tfrac{7}{3}|\mathcal{M}^{(+)}|^2+3|\mathcal{M}^{(-)}|^2\ . \tag{B10}$$

APPENDIX C

This appendix describes how cross sections are calculated from the amplitudes given in Sec. II and fixes our normalization conventions for phase-space integrals, states, etc. The amplitudes presented describe more than 100 different processes at e^+e^-, $e^\pm p$, and hadron colliders, even when scattering processes involving different flavors are not counted. Of course, most of them are related by crossing, and in order to specify a given process one merely has to state which momenta are incoming and which are outgoing; i.e., one has to fix the sign factors relating the physical momenta $\bar{p}_i,\bar{g}_i,\bar{l}_i$ (with positive time component) to the momenta p_i,g_i,l_i used in the amplitude formulas:

$$\begin{aligned}&\text{quarks:}\quad p_i=S_i\bar{p}_i\ ,\\ &\text{gluons:}\quad g_i=r_i\bar{g}_i\ ,\\ &\text{leptons:}\quad l_i=s_i\bar{l}_i\ .\end{aligned} \tag{C1}$$

The sign factors can be summarized as follows: for quarks and leptons, $S_i,s_i=+$; for antiquarks and antileptons, $S_i,s_i=-$; for gluon in final state, $r_i=+$; for gluon in initial state, $r_i=-$.

For virtual vector bosons, the boson polarization vectors must be replaced by the decay currents as indicated in Eq. (2.29). The amplitudes given in Sec. II are for fixed polarizations of the external particles and have the general form

$$\mathcal{M}=\sum_m\mathcal{M}^{(m)}\mathcal{O}^{(m)}\ , \tag{C2}$$

where the $\mathcal{O}^{(m)}$ are orthogonal color tensors. After fixing the sign factors, the sum over colors is common to all the processes that are related by crossing

$$\sum_{\text{colors}}|\mathcal{M}|^2=\sum_m c_m|\mathcal{M}^{(m)}|^2\ , \tag{C3}$$

with the weights c_m given by Eqs. (B2), (B3), (B9), and (B10). For any process the parton-level differential cross section assumes the generic form

$$d\hat{\sigma}=\frac{1}{2\hat{s}}\frac{1}{4}A_cF_S\sum_{\text{flavors}}\sum_{\bar{\rho}_1,\bar{\rho}_3}\sum_{\bar{\sigma}_1,\bar{\sigma}_3}\sum_{\bar{\kappa}_1,\bar{\kappa}_2}\sum_m c_m|\mathcal{M}^{(m)}|^2d\phi_n\ . \tag{C4}$$

The factors appearing above are explained in the following

$\frac{1}{4}$: average over initial-state helicities.

A_c: average over initial-state colors. A_c contains a factor 1, $\frac{1}{3}$, $\frac{1}{8}$ for each incoming electron, quark, gluon.

F_S: the statistical factor for identical particles in the final state. A factor $\frac{1}{2}$ for every pair of identical quarks, $\frac{1}{2}$ for every pair of identical antiquarks, $1/k!$ for k gluons, and $\frac{1}{2}$ for a pair of identical electroweak bosons. In the prescription for treating electroweak-boson decay in Sec. II E the amplitudes are *not* antisymmetrized in identical decay leptons arising from the decay of different electroweak bosons, and hence no factors of $\frac{1}{2}$ should be included for identical leptons or antileptons in the final state.

Σ_{flavors}: summation over different quark flavors in the final state which given rise to the same experimental signature.

$\Sigma_{\bar{\rho}_1,\bar{\rho}_3}$: summation over lepton helicities. This sum is to be replaced by a sum over electroweak-boson polarizations if the bosons are not decayed.

$\Sigma_{\bar{\sigma}_1,\bar{\sigma}_3}$: summation over quark polarizations. Notice that the Kronecker deltas $\delta_{\sigma_1\sigma_2}\delta_{\sigma_3\sigma_4}$ or $\delta_{\sigma_1\sigma_4}\delta_{\sigma_3\sigma_2}$, which arise from chirality conservation, are already taken into account, and the helicities $\bar{\sigma}_2$ and $\bar{\sigma}_4$ are determined uniquely in terms of $\bar{\sigma}_1$ and $\bar{\sigma}_3$.

$\Sigma_{\bar{\kappa}_1,\bar{\kappa}_2}$: summation over gluon polarizations.

$d\phi_n$: n-body Lorentz-invariant phase-space element. The amplitudes are normalized such that for any process involving bosons and fermions, the n-body phase-space element is

$$d\phi_n=(2\pi)^4\delta^4\left[\bar{P}-\sum_{j=1}^{n}\bar{p}_j\right]\prod_{i=1}^{n}\frac{d^3\bar{p}_i}{(2\pi)^3 2\bar{p}_i^0}\ , \qquad \text{(C5)}$$

where $\bar{P}$ denotes the total incoming four-momentum and $\bar{p}_i^{\mu}$ $(i,1,\ldots,n)$ denote n final-state four-momenta.

The phase-space integration will usually be done by Monte Carlo integration. When dealing with more than 2 or 3 particles in the final state, it may be advantageous to perform the polarization sums by Monte Carlo integration as well. For $q\bar{q}\rightarrow ggZZ$, for example, this means that each event requires the evaluation of the matrix element for one fixed set of polarization indices only. A direct summation over polarizations would require $2^3 3^2=72$ evaluations for each flavor combination and may hence reduce the speed of the program significantly. The Monte Carlo approach simply simulates reality, where the sum/average over different polarizations is obtained only statistically.

[1]V. Barger and R. J. N. Phillips, *Collider Physics* (Frontiers in Physics, Vol. 71) (Addison-Wesley, Reading, MA, 1987); in *Proceedings of the Workshop on Physics at Future Accelerators,* La Thuile, Italy, 1987, edited by J. H. Mulvey (CERN Report No. 87-07, Geneva, Switzerland, 1987).

[2]E. Eichten, I. Hinchliffe, K. Lane, and C. Quigg, Rev. Mod. Phys. **56**, 579 (1984); **58**, 1065(E) (1986).

[3]K. Hagiwara, R. D. Peccei, D. Zeppenfeld, and K. Hikasa, Nucl. Phys. **B282**, 253 (1987), and references therein.

[4]R. W. Brown and K. O. Mikaelian, Phys. Rev. D **19**, 922 (1979); R. W. Brown, D. Sahdev, and K. O. Mikaelian, *ibid.* **20**, 1164 (1979); J. Stroughair and C. L. Bilchak, Z. Phys. C **23**, 377 (1984); M. J. Duncan, G. L. Kane, and W. W. Repko, Nucl. Phys. **B272**, 517 (1986); S.-C. Lee and W.-C. Su, Phys. Lett. B **212**, 113 (1988).

[5]C. H. Llewellyn Smith and B. H. Wiik, Report No. DESY 77/38, 1977 (unpublished); P. Salati and J. C. Wallet, Z. Phys. C **16**, 155 (1982); A. N. Kamal *et al.*, Phys. Rev. D **24**, 2842 (1981); H. Neufeld, Z. Phys. C **17**, 145 (1983); G. Altarelli *et al.*, Nucl. Phys. **B262**, 204 (1985).

[6]K. Hagiwara and D. Zeppenfeld, Nucl. Phys. **B313**, 560 (1989).

[7]F. A. Berends, W. T. Giele, and H. Kuijf, Nucl. Phys. **B321**, 39 (1989).

[8]V. Barger, T. Han, J. Ohnemus, and D. Zeppenfeld, Phys. Rev. Lett. **62**, 1971 (1989); Phys. Rev. D **40**, 2888 (1989); Phys. Lett. B **232**, 371 (1989).

[9]F. A. Berends, W. T. Giele, H. Kuijf, R. Kleiss, and W. J. Stirling, Phys. Lett. B **224**, 237 (1989).

[10]C.-H. Chang and S.-C. Lee, Phys. Rev. D **37**, 101 (1988); D. Zeppenfeld and S. Willenbrock, *ibid.* **37**, 1775 (1988); U. Baur and D. Zeppenfeld, Nucl. Phys. **B308**, 127 (1988); K. Hagiwara, J. Woodside, and D. Zeppenfeld, Phys. Rev. D **41**, 2113 (1990).

[11]E. Gabrielli, Mod. Phys. Lett A **1**, 465 (1986); M. Böhm and A. Rosado, Z. Phys. C **39**, 275 (1988); **42**, 479 (1989); U. Baur and D. Zeppenfeld, Nucl. Phys. **B325**, 253 (1989).

[12]P. Aurenche, A. Douiri, R. Baier, M. Fontannaz, and D. Schiff, Z. Phys. C **29**, 459 (1985).

[13]J. Smith, D. Thomas, and W. L. van Neerven, Z. Phys. C **44**, 267 (1989).

[14]U. Baur, E. W. N. Glover, and J. J. van der Bij, Nucl. Phys. **B318**, 106 (1989).

[15]For recent analyses see, e.g., H. Baer, V. Barger, and R. J. N. Phillips, Phys. Lett. B **221**, 398 (1989); Phys. Rev. D **39**, 3310 (1989); H. Baer, V. Barger, H. Goldberg, and R. Phillips, *ibid.* **37**, 3152 (1988); R. Kleiss, A. D. Martin, and W. J. Stirling, Z. Phys. C **39**, 393 (1988); J. Rosner, Phys. Rev. D **39**, 3297 (1989); **40**, 1701(E) (1989); P. Agrawal and S. D. Ellis, Phys. Lett. B **221**, 393 (1989); W. T. Giele and W. J. Stirling, Leiden Report No. 89-0634, 1989 (unpublished).

[16]R. N. Cahn, S. D. Ellis, R. Kleiss, and W. J. Stirling, Phys. Rev. D **35**, 1626 (1987); R. Kleiss and W. J. Stirling, Phys. Lett. B **200**, 193 (1988); V. Barger, T. Han, and R. J. N. Phillips, Phys. Rev. D **37**, 2005 (1988).

[17]H. Baer, V. Barger, D. Karatas, and X. Tata, Phys. Rev. D **36**, 96 (1987); H. Baer *et al.*, Int. J. Mod. Phys. A **2**, 1131 (1987); J. F. Gunion *et al.*, *ibid.* **2**, 1145 (1987); R. M. Barnett *et al.*, in *Proceedings of the Workshop on Experiments, Detectors, and Experimental Areas for Supercollider,* Berkeley, California, 1987, edited by R. Donaldson and M. Gilchriese (World Scientific, Singapore, 1988), p. 178.

[18]J. F. Gunion, J. Kalinowski, and A. Tofighi-Niaki, Phys. Rev. Lett. **57**, 2351 (1986); D. A. Dicus and R. Vega, Phys. Lett. B **217**, 194 (1989).

[19]P. De Causmaeker, R. Gastmans, W. Troost, and T. T. Wu, Nucl. Phys. **B206**, 53 (1982); F. A. Berends, R. Kleiss, P. De Causmaeker, R. Gastmans, W. Troost, and T. T. Wu, *ibid.* **B206**, 61 (1982); **B264**, 265 (1986), and references therein; D. Danckaert, P. De Causmaeker, R. Gastmans, W. Troost, and T. T. Wu, Phys. Lett. **114B**, 203 (1982).

[20]Z. Xu, Da-Hua Zhang, and L. Chang, Tsinghua University, Beijing, Reports Nos. TUTP-84/4, TUTP-84/5, TUTP-84/6 (unpublished); Nucl. Phys. **B291**, 392 (1987); J. F. Gunion and Z. Kunszt, Phys. Lett. **161B**, 333 (1985); R. Kleiss and W. J. Stirling, Nucl. Phys. **B262**, 167 (1985).

[21]T. B. Anders and W. Jachmann, J. Math. Phys. **24**, 2847 (1983); **28**, 221 (1987).

[22]K. Hagiwara and D. Zeppenfeld, Nucl. Phys. **B274**, 1 (1986); **B313**, 560 (1989).

[23]CDF Collaboration, F. Abe *et al.*, Phys. Rev. Lett. **63**, 720 (1989).

[24]Mark II Collaboration, G. S. Abrams *et al.*, Phys. Rev. Lett. **63**, 724 (1989).

[25]ALEPH Collaboration, D. Decamp *et al.*, Phys. Lett. B **231**, 519 (1989); **235**, 399 (1990); DELPHI Collaboration, P. Aarnio *et al.*, *ibid.* **231**, 539 (1989); L3 Collaboration, B. Adeva *et al.*, *ibid.* **231**, 509 (1989); OPAL Collaboration, M. Z. Akrawy *et al.*, *ibid.* **231**, 530 (1989).

[26]K. O. Mikaelian, M. A. Samuel, and D. Sahdev, Phys. Rev. Lett. **43**, 746 (1979); D. Zhu, Phys. Rev. D **22**, 2266 (1980); C. J. Goebel, F. Halzen, and J. P. Leveille, *ibid.* **23**, 2682 (1981); S. J. Brodsky and R. W. Brown, Phys. Rev. Lett. **49**, 966 (1982); M. A. Samuel, Phys. Rev. D **27**, 2724 (1983); R. W. Brown, K. L. Kowalski, and S. J. Brodsky, *ibid.* **28**, 624

(1983); J. Cortés, K. Hagiwara, and F. Herzog, Nucl. Phys. **B278**, 26 (1986); M. A. Samuel and J. H. Reid, Prog. Theor. Phys. **76**, 184 (1986).

[27]B. L. Combridge, Nucl. Phys. **B174**, 243 (1980); C. Carimalo *et al.*, Phys. Lett. **98B**, 105 (1981); E. L. Berger, E. Braaten, and R. D. Field, Nucl. Phys. **B239**, 52 (1984).

[28]E. W. N. Glover and J. J. van der Bij, Phys. Lett. B **206**, 701 (1988); Nucl. Phys. **B219**, 488 (1989); **B321**, 561 (1989).

[29]V. Barger, T. Han, J. Ohnemus, and D. Zeppenfeld (in preparation).

[30]D. Zeppenfeld, Int. J. Mod. Phys. A **3**, 2175 (1988).